Data in Brief 35 (2021) 106854

Contents lists available at ScienceDirect

Data in Brief

journal homepage: www.elsevier.com/locate/dib

Data Article

Big Data acquired by Internet of Things-enabled industrial multichannel wireless sensors networks for active monitoring and control in the smart grid Industry 4.0

Muhammad Faheem[a,b,*], Ghulam Fizza[c], Muhammad Waqar Ashraf[d], Rizwan Aslam Butt[e], Md. Asri Ngadi[a], Vehbi Cagri Gungor[b]

[a] Department of Computer Science, Universiti Teknologi Malaysia, Johor Bahru 801310, Malaysia
[b] Department of Computer Engineering, Abdullah Gul University, Kayseri 38080, Turkey
[c] Department of Telecommunication Engineering, Quaid-e-Awam University of Engineering Science and Technology, Nawabshah 67450, Sindh, Pakistan
[d] Department of Computer Engineering, Bahauddin Zakariya University, Multan 60800, Pakistan
[e] Department of Electronics Engineering, NED University, Karachi 75270, Pakistan

ARTICLE INFO

Article history:
Received 19 December 2020
Revised 14 January 2021
Accepted 4 February 2021
Available online 6 February 2021

Keywords:
Internet of things
Wireless sensor networks
Multichannel wireless sensor network
Smart grid
Industry 4.0

ABSTRACT

Smart Grid Industry 4.0 (SGI4.0) defines a new paradigm to provide high-quality electricity at a low cost by reacting quickly and effectively to changing energy demands in the highly volatile global markets. However, in SGI4.0, the reliable and efficient gathering and transmission of the observed information from the Internet of Things (IoT)-enabled Cyber-physical systems, such as sensors located in remote places to the control center is the biggest challenge for the Industrial Multichannel Wireless Sensors Networks (IMWSNs). This is due to the harsh nature of the smart grid environment that causes high noise, signal fading, multipath effects, heat, and electromagnetic interference, which reduces the transmission quality and trigger errors in the IMWSNs. Thus, an efficient monitoring and real-time control of unexpected

* Corresponding author at: Department of Computer Science, Universiti Teknologi Malaysia, Johor Bahru 801310, Malaysia.
E-mail address: muhammad.faheem@agu.edu.tr (M. Faheem).

https://doi.org/10.1016/j.dib.2021.106854

changes in the power generation and distribution processes is essential to guarantee the quality of service (QoS) requirements in the smart grid. In this context, this paper describes the dataset contains measurements acquired by the IMWSNs during events monitoring and control in the smart grid. This work provides an updated detail comparison of our proposed work, including channel detection, channel assignment, and packets forwarding algorithms, collectively called CARP [1] with existing G-RPL [2] and EQSHC [3] schemes in the smart grid. The experimental outcomes show that the dataset and is useful for the design, development, testing, and validation of algorithms for real-time events monitoring and control applications in the smart grid.

Specifications Table

Subject	Computer Networks and Communication, Engineering.
Specific subject area	MWSNs communication in the smart grid
Type of data	Tables and Graphs
How data were acquired	Data was captured using sensors in the 500kV outdoor power grid station
Data format	Raw and analysed sensor data in the smart grid
Description of data collection	The data were gathered using sensors in the smart grid environment containing various systems or subsystems and electric poles with values 160 and 120, respectively. In order to gather data in different scenarios, random topologies were considered within the smart grid environment. In the meanwhile, a static sink was deployed near the sensors to collect real-time data in the smart grid. The remote user can access and configure each sensor by connecting to the sink and the base station using wired or wireless intranet and internet communication technologies.
Parameters for data collection	The data were collected during the day using 300 sensors, each of them equipped with physical layer standard 802.11g, the frequency range between 2.412GHz and 2.484GHz with random topology in the power grid.
Data source location	City/Town/Region: Kayseri, Country: Turkey.
Related research article	The updated data is related to the research article presented in [1].
Data accessibility	Data is provided within this article and, Data Repository name: Mendeley Direct URL to data: https://dx.doi.org/10.17632/32d6r6r6zk.1

Value of the Data

- The data provided in this paper provides can be used for efficient monitoring and control of the power generation and distribution processes in the smart grid.
- The data provided in this paper can be used for the integration of distributed power generation sources into the power transmission and distribution systems within realistic network scenarios.
- It can also support reliable and dynamic data capacity requirements of different types of advanced cyber-physical systems equipped with sensors and devices to operate them optimally, either manual or automatic controls, and provide information about their operations to the utilities.

- In case of faults, the designed scheme intelligently monitoring and identifies the faulty systems located in a remote position and notifies the user in real-time, so that appropriate actions can be taken to supply steady electricity to the customers.

1. Data Description

The dataset provided in this paper offers valuable information for efficient monitoring and control of the power generation and distribution processes in the smart grid. The advantage of these data is to provide intelligently monitoring and identifies the faulty systems located in the remote positions to notify the user in real-time so that appropriate actions can be taken to supply steady electricity to the customers. The data provided in this article were gathered using multichannel wireless sensor nodes located at remote locations in an outdoor power generation and distribution centers in the smart grid. In the smart grid, each node by following an event-driven or query-based information gathering model monitors the surrounding, collaborates with each other, and reports the sensed data to the sink. The user using IoS via IoT can directly monitor, control, and configure any deployed sensor node through the base station and the sink as shown in Fig. 1 [1].

In Fig. 1, the black colored icons are the wireless sensor nodes. The unique number on the right side of each sensor node shows the identity in the network. The device equipped with dual antennas on the right side of the deployed network is the sink while the pole like icon is the BS. The orange-colored thick multiple lines generate the same inference level, such as systems, subsystems, and electric poles in the SG. The thin orange-colored lines on the left and right sides defined the network boundary. The blue-colored circular line shows the sink range for message transmission and reception in the network. The black line between the sink and the base station and the base station to the user shows the highly stable bi-directional communication links in the network. The cloud-like icon indicates the network is either a LAN, NAN, or WAN.

Table 1 and Table 2 present the data of the probability of channel detection and the probability of false alarms in the MWSNs. Fig. 2 portrays the trends of both probabilities of channel detection and false alarms in the MWSNs. Table 3 describes the data values of the probability

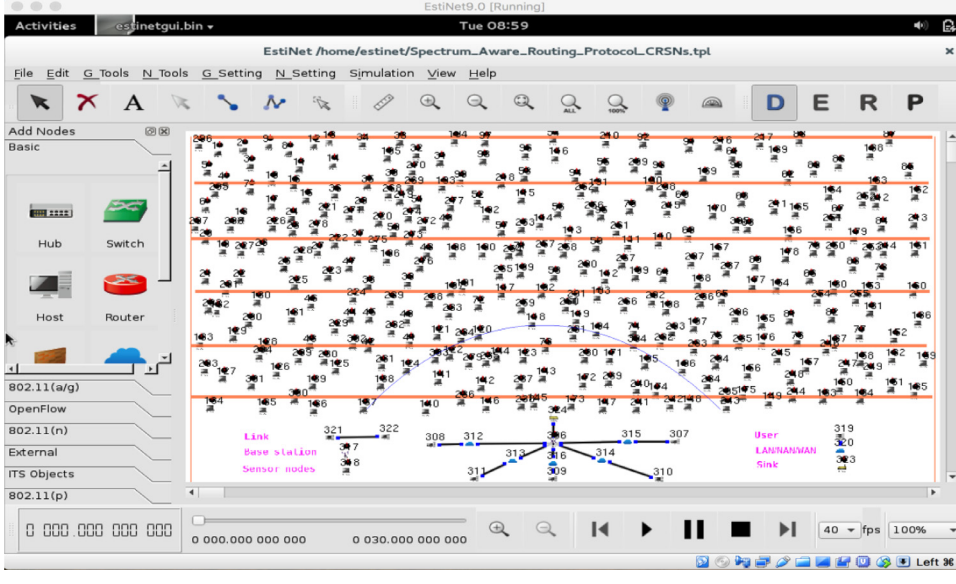

Fig. 1. A view of the network model in the smart grid.

Table 1
The probability of channel detection values in MWSNs.

No. of rounds	Probability of channel detection values					
Protocols	CARP	Avg. (≅)	G-RPL	Avg. (≅)	EQSHC	Avg. (≅)
100	0.9250		0.8550		0.7880	
200	0.9280		0.8680		0.7780	
300	0.9190		0.8300		0.7630	
400	0.9300		0.8390		0.7570	
500	0.9190		0.8220		0.7480	
600	0.9180		0.8310		0.7290	
700	0.9240		0.8610		0.7250	
800	0.9320		0.8990		0.7610	
900	0.9350		0.8400		0.7390	
1000	0.9330		0.8580		0.7470	
1100	0.9290		0.8590		0.7710	
1200	0.9190		0.8300		0.7390	
1300	0.9390		0.8290		0.7710	
1400	0.9190		0.8320		0.7480	
1500	0.9180	93.6%	0.8510	85%	0.7290	76%
1600	0.9240		0.8610		0.7250	
1700	0.9290		0.8490		0.7610	
1800	0.9390		0.8500		0.7790	
1900	0.9310		0.8480		0.7770	
2000	0.9320		0.8690		0.7810	
2100	0.9300		0.8300		0.7690	
2200	0.9310		0.8490		0.7810	
2300	0.9300		0.8500		0.7590	
2400	0.9280		0.8580		0.7470	
2500	0.9220		0.8720		0.7590	
2600	0.9290		0.8790		0.7510	
2700	0.9390		0.8600		0.7390	
2800	0.9280		0.8580		0.7470	
2900	0.9280		0.8680		0.7470	
3000	0.9320		0.8420		0.7590	

Table 2
The probability of missed-detection values in MWSNs.

No. of rounds	Probability of missed-detection values					
Protocols	CARP	Avg. (≅)	G-RPL	Avg. (≅)	EQSHC	Avg. (≅)
100	0.3380		0.5280		0.9050	
200	0.3290		0.5210		0.9040	
300	0.3340		0.5180		0.9240	
400	0.3990		0.5600		0.9110	
500	0.3160		0.5710		0.9020	
600	0.3150		0.5350		0.9080	
700	0.3250		0.5800		0.8950	
800	0.3340		0.5780		0.8970	
900	3.2980		0.5670		0.9000	
1000	0.3980		0.5600		0.9100	
1100	0.3040		0.5480		0.9170	
1200	0.3290		0.5670		0.9090	
1300	0.3040		0.5480		0.9190	
1400	0.3160		0.5490		0.9180	
1500	0.2990	3.3%	0.5550	5.5%	0.9180	9%
1600	0.3280		0.5400		0.9080	
1700	0.3440		0.5380		0.9000	
1800	0.3190		0.5570		0.9110	
1900	0.3110		0.5500		0.8910	
2000	0.3240		0.5380		0.8990	

(*continued on next page*)

Table 2 (*continued*)

No. of rounds	Probability of missed-detection values					
Protocols	CARP	Avg. (≅)	G-RPL	Avg. (≅)	EQSHC	Avg. (≅)
2100	0.3290		0.5470		0.9050	
2200	0.3340		0.5380		0.9090	
2300	0.3390		0.5670		0.9950	
2400	0.3280		0.5400		0.8900	
2500	0.3290		0.5300		0.9000	
2600	0.3340		0.5680		0.9090	
2700	0.3390		0.5620		0.8970	
2800	0.3380		0.5600		0.9020	
2900	0.3310		0.5500		0.9100	
3000	0.3300		0.5530		0.9140	

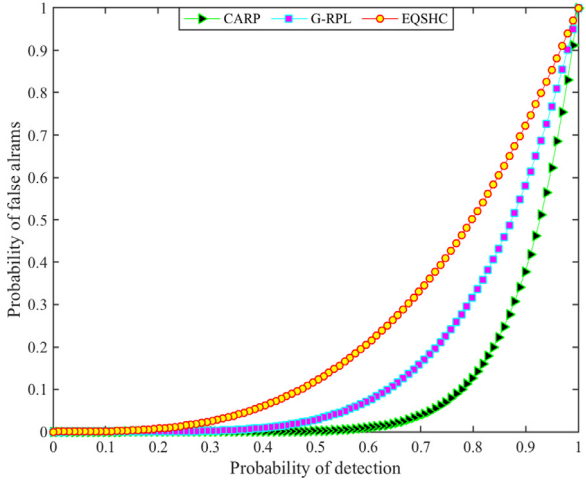

Fig. 2. The probability of false alarms and probability of detection.

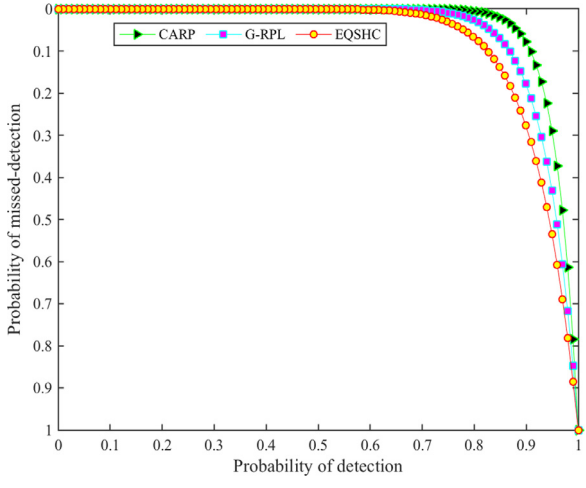

Fig. 3. The probability of missed-detection and probability of detection.

Table 3
The probability of false alarm values in MWSNs.

No. of rounds	Probability of false alarms values					
Protocols	CARP	Avg. (≅)	G-RPL	Avg. (≅)	EQSHC	Avg. (≅)
100	0.3110		0.9710		0.1470	
200	0.2370		0.8610		0.1530	
300	0.3360		0.8580		0.1670	
400	0.3420		0.9930		0.1530	
500	0.3350		0.8510		0.1770	
600	0.3380		0.9430		0.1270	
700	0.2430		0.8480		0.1380	
800	0.2460		0.8890		0.1490	
900	0.3390		0.9930		0.1850	
1000	0.2370		0.8710		0.1540	
1100	0.3460		0.7890		0.1470	
1200	0.2390		0.7950		0.1350	
1300	0.3460		0.8810		0.1490	
1400	0.3350		0.7510		0.1610	
1500	0.3380	3.1%	0.8460	9.5%	0.1760	15%
1600	0.2430		0.8480		0.1420	
1700	0.3460		0.9860		0.1490	
1800	0.2390		0.8910		0.1350	
1900	0.3370		0.9740		0.1530	
2000	0.3460		0.7890		0.1490	
2100	0.3390		0.8950		0.1350	
2200	0.3460		0.7850		0.1480	
2300	0.3390		0.8950		0.1350	
2400	0.2370		0.9740		0.1540	
2500	0.3400		0.9690		0.1440	
2600	0.3460		0.8830		0.1490	
2700	0.3390		0.8950		0.1350	
2800	0.3370		0.9740		0.1540	
2900	0.2370		0.9740		0.1530	
3000	0.2400		0.8610		0.8400	

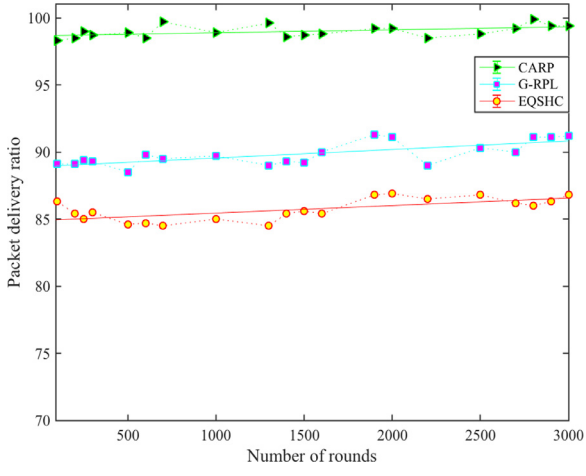

Fig. 4. The packet delivery ratio vs number of rounds between 1 and 3000.

Table 4
The packet delivery ratio values in MWSNs.

No. of rounds	Packet delivery ratio values					
Protocols	CARP	Avg. (≅)	G-RPL	Avg. (≅)	EQSHC	Avg. (≅)
100	0.9830		0.8910		0.8630	
200	0.9850		0.8910		0.8540	
300	0.9900		0.8940		0.8560	
400	0.9900		0.8860		0.8440	
500	0.9910		0.8910		0.8460	
600	0.9890		0.8980		0.8450	
700	0.9970		0.8970		0.8490	
800	0.9960		0.9200		0.8460	
900	0.9950		0.9290		0.8530	
1000	0.9930		0.8970		0.8570	
1100	0.9960		0.9160		0.8560	
1200	0.9890		0.9290		0.8520	
1300	0.9970		0.8920		0.8450	
1400	0.9920		0.8940		0.8540	
1500	0.9930	99.5%	0.8920	92%	0.8560	86.7%
1600	0.9930		0.9000		0.8540	
1700	0.9940		0.9060		0.8610	
1800	0.9900		0.9090		0.8600	
1900	0.9940		0.9130		0.8680	
2000	0.9940		0.9110		0.8690	
2100	0.9930		0.9090		0.8390	
2200	0.9900		0.8900		0.8650	
2300	0.9910		0.9280		0.8490	
2400	0.9920		0.9250		0.8630	
2500	0.9910		0.9030		0.8680	
2600	0.9930		0.8900		0.8600	
2700	0.9930		0.9000		0.8620	
2800	0.9970		0.9210		0.8600	
2900	0.9950		0.9210		0.8630	
3000	0.9950		0.9220		0.8680	

of missed-detection in the MWSNs. Fig. 3 presents the trends of the probability of channel detection and the probability of missed-detection in the MWSNs. Table 4 describes the packet delivery ratio data values while the graph in Fig. 4 presents the trends of packet delivery ratio in the MWSNs. Table 5 describes the latency data values in the MWSNs. Fig. 5 presents the trends of latency in the MWSNs. Table 6 describes the packet error rate data values while the graph in Fig. 6 shows the trends of the packet error rate in the MWSNs. Finally, Table 7 shows the congestion management data values and Fig. 7 presents the trends of congestion management values in the MWSNs.

2. Experimental Design, Materials and Methods

In this study, we consider a 550 kV outdoor grid station with an area of 1100 (length) × 700 (width) meters containing 300 wireless sensors in the network. The grid contains power generation and distribution systems and subsystem, and electric poles with numbers 160 and 120, respectively. The initial energy of each wireless sensor is set to 5J in the MWSNs. In the MWSNs, each wireless sensor is embedded with physical layer standard IEEE 802.11g with a maximum communication range up to 85 m and data rates up to 256kbps. The IEEE 802.11g standard offers a total number of 12 channels in the 2.4GHz band, in which three, 1, 6, 11, are non-overlapping channels.

Consequently, each sensor is embedded with multiple radios and a single interface, where each radio at a given time serves as a receiver or a transmitter for the distinct channel, i.e., half-

Table 5
The latency values in MWSNs.

No. of nodes	Latency values					
Protocols	CARP	Avg. (≅)	G-RPL	Avg. (≅)	EQSHC	Avg. (≅)
10	0.3000		0.3200		0.4900	
20	0.4500		0.6800		0.5400	
30	0.5700		0.8800		0.7100	
40	0.6400		0.1400		0.8000	
50	0.7500	77.5%	0.1600	201.8%	0.9900	140.7%
60	0.8700		0.1970		0.1120	
70	0.9500		0.2560		0.1390	
80	0.9900		0.2630		0.1050	
90	1.0800		0.2890		0.1910	
100	1.1500		0.3010		0.2100	
110	0.1400		0.3180		0.2270	
120	0.1800		0.3290		0.2410	
130	0.1980		0.3450		0.2720	
140	0.2100		0.3590		0.2980	
150	0.2200	226.7%	0.3730	418.20%	0.3200	379.54%
160	0.2230		0.3810		0.3350	
170	0.2260		0.4390		0.3490	
180	0.2600		0.4620		0.3680	
190	0.2900		0.4770		0.3810	
200	0.3200		0.4910		0.3870	
210	0.3240		0.4990		0.3990	
220	0.3300		0.5420		0.4200	
230	0.3410		0.5710		0.4620	
240	0.3640		0.5800		0.4750	
250	0.3800	398.7%	0.6077	543.6%	0.4990	479.32%
260	0.3970		0.6130		0.5340	
270	0.4370		0.6380		0.5470	
280	0.4630		0.6690		0.5630	
290	0.4710		0.6888		0.5820	
300	0.4800		0.6940		0.5980	

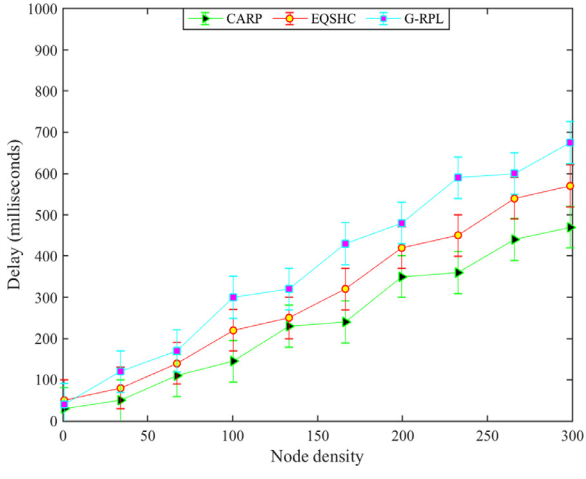

Fig. 5. The network delay vs number of sensor nodes between 1 and 300.

Table 6
The packet error rate values in MWSNs.

No. of nodes	Packet error rate values					
Protocols	CARP	Avg. (≅)	G-RPL	Avg. (≅)	EQSHC	Avg. (≅)
10	0.0100		0.0500		0.0490	
20	0.0900		0.4250		0.2480	
30	0.1800		0.3180		0.0680	
40	0.1600		0.5100		0.0470	
50	0.0600	1.1%	0.3890	3.88%	0.0670	1.8%
60	0.1200		0.3870		0.2890	
70	0.1500		0.3860		0.1990	
80	0.1300		0.3850		0.3850	
90	0.0940		0.4990		0.3710	
100	0.0530		0.5300		0.0780	
110	0.2280		0.6080		0.3470	
120	0.2150		0.7690		0.3510	
130	0.2170		0.8800		0.4220	
140	0.1700		0.9020		0.5080	
150	0.1850	1.89%	0.9310	9.3%	0.6890	6.8%
160	0.1600		0.9810		0.7990	
170	0.1800		1.2900		0.8710	
180	0.1700		0.9020		0.9400	
190	0.1800		0.9310		0.9290	
200	0.1900		1.1810		0.8980	
210	0.2790		0.8999		0.5910	
220	0.2590		0.9380		0.8700	
230	0.3310		1.3030		0.8820	
240	0.3440		1.3270		0.9750	
250	0.1660	2.8%	1.3180	12.6%	0.9710	9.3%
260	0.2990		1.2991		0.7990	
270	0.2870		1.3180		1.2170	
280	0.2590		1.2990		1.1110	
290	0.2790		1.4370		0.9830	
300	0.2850		1.4390		0.9920	

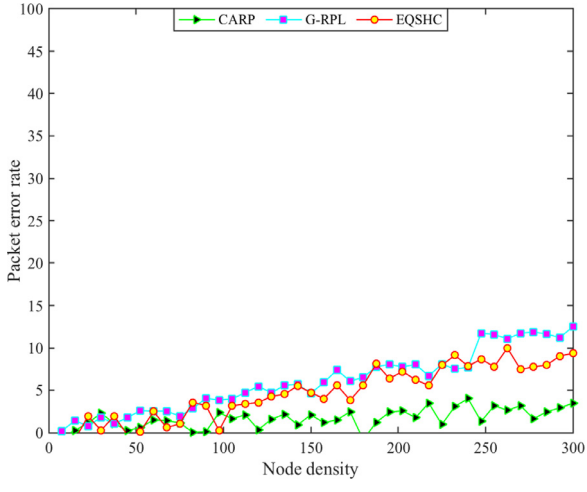

Fig. 6. The packet error rate vs number of nodes between 1 and 300.

Table 7
The congestion management values in MWSNs.

No. of nodes	Congestion management values					
Protocols	CARP	Avg. (≅)	G-RPL	Avg. (≅)	EQSHC	Avg. (≅)
10	0.9950		0.9700		0.9900	
20	0.9940		0.9650		0.9870	
30	0.9910		0.9560		0.9850	
40	0.9900		0.9480		0.9810	
50	0.9850	98.07%	0.9450	94.45%	0.9780	97.06%
60	0.9830		0.9430		0.9750	
70	0.9770		0.9350		0.9630	
80	0.9700		0.9300		0.9600	
90	0.9660		0.9290		0.9560	
100	0.9560		0.9240		0.9310	
110	0.9510		0.9200		0.9180	
120	0.9460		0.9160		0.9060	
130	0.9300		0.9090		0.8970	
140	0.9300		0.8940		0.8850	
150	0.9250	93.02%	0.8900	89.25%	0.8800	87.99%
160	0.9240		0.8860		0.8780	
170	0.9260		0.8820		0.8760	
180	0.9240		0.8800		0.8650	
190	0.9220		0.8750		0.8530	
200	0.9240		0.8730		0.8410	
210	0.9230		0.8710		0.8360	
220	0.9230		0.8720		0.8250	
230	0.9230		0.8700		0.8200	
240	0.9210		0.8660		0.8190	
250	0.9230	92.20%	0.8560	84.59%	0.8110	81.66%
260	0.9240		0.8490		0.8030	
270	0.9220		0.8300		0.7990	
280	0.9210		0.8260		0.7880	
290	0.9200		0.8190		0.8850	
300	0.9202		0.8000		0.7800	

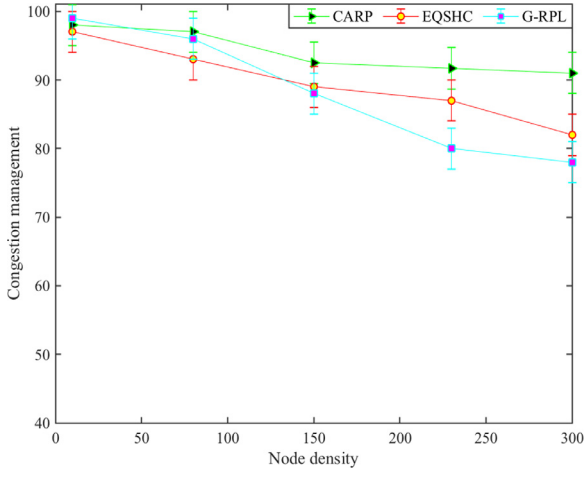

Fig. 7. The congestion management vs node density between 1 and 300.

Table 8
Simulation parameters and values.

Simulation Model Parameters	Values
Wireless sensors	300
Physical layer standard	802.11g
Frequency	2.412GHz to 2.484GHz
Number of channels	12
Non-overlapping channels	1,6,11
Initial sensor node energy	5J
High transmission power	0.97W
Low transmission power	0.82W
Packet receiving power	0.05W
Ideal listening	0.023W
Sleeping power	3×10^{-6}W
Data aggregation	0.019W
Packet length	43bytes
Data transfer rate	256 kbps
Cache	2Mb
Maximum hop distance	85m
Maximum communication range of the sink	150m
Topology	Random
Antenna	Omni-directional
Path loss exponent for the line of sight and non-line-of-sight	2.4, 3.5
The noise floor for the line of sight and non-line-of-sight	–83, –91
Shadowing deviation for the line of sight and non-line-of-sight	3.12, 2.92
Systems, subsystems, and poles in the grid	160, 120
Area: 2D (length $\times$ width)	1100 $\times$ 700m
Simulation time	120 sec
Set of simulations	53

duplex mode. The number of available channels on each sensor is equal to the number of radios in MWSNs. Each sensor is equipped with a control channel as a default channel that is always in the receiving mode and can transmit control messages to its neighbors on-demand in a specific deployed area in the network. The Quadrature phase-shift keying (QPSK) modulation technique was assumed and the value of data packet size was set to 43 bytes in the network [3-5]. During the network operations, each wireless sensor observes the grid events and stores data in its memory of the maximum size of 2Mb. In the packet transmission process, the maximum value of energy consumed for transmitting with high and low power was set to 0.97W and 0.82W, while the energy consumed upon receiving data is set to 0.05W in the network.

The values of ideal listening and sleeping power were set to 0.023 W and 3×10^{-6}W, respectively. Finally, 53 sets of simulations were performed to provide consistent results of the proposed scheme against the existing schemes in the network. The widely used simulation parameters and their values used in our study are given in Table 8 [6-10].

Declaration of Competing Interest

The authors declare that they have no known competing financial interests or personal relationships that could have appeared to influence the work reported in this paper.

Acknowledgments

This research has been supported by the Universiti Teknologi Malaysia (UTM), IDF-UTM.J.10.01/13.14/1/128 (201801M10702).

References

[1] M. Faheem, R.A. Butt, B. Raza, M.W. Ashraf, M.A. Ngadi, V.C. Gungor, A multi-channel distributed routing scheme for smart grid real-time critical event monitoring applications in the perspective of Industry 4.0, Int. J. Ad Hoc Ubiquit. Comput. 32 (4) (2019) 236–256.
[2] Z. Yang, R. Han, Y. Chen, X. Wang, Green-RPL: an energy-efficient protocol for cognitive radio enabled AMI network in smart grid, IEEE Access 6 (2018) 18335–18344.
[3] E. Fadel, et al., Spectrum-aware bio-inspired routing in cognitive radio sensor networks for smart grid applications, Comput. Commun. 101 (2017) 106–120.
[4] S.B. Shah, et al., 3D weighted centroid algorithm & RSSI ranging model strategy for node localization in WSN based on smart devices, Sustain. Cities Soc. 39 (2018) 298–308.
[5] M.Z. Abbas, et al., Key factors involved in pipeline monitoring techniques using robots and WSNs: Comprehensive survey, J. Pipeline Syst. Eng. Pract. 9 (2) (2018) 04018001.
[6] M. Faheem, V. Gungor, MQRP: Mobile sinks-based QoS-aware data gathering protocol for wireless sensor network-s-based smart grid applications in the context of industry 4.0-based on internet of things, Fut. Gen. Comput. Syst. (2017).
[7] M. Faheem and V. C. Gungor, "Energy efficient and QoS-aware routing protocol for wireless sensor network-based smart grid applications in the context of industry 4.0," *Appl. Soft Comput.*,2017/07/27/2017.
[8] V.C. Gungor, D. Sahin, Cognitive radio networks for smart grid applications: a promising technology to overcome spectrum inefficiency, IEEE Veh. Technol. Mag. 7 (2) (2012) 41–46.
[9] M. Faheem, M.Z. Abbas, G. Tuna, V.C. Gungor, EDHRP: Energy efficient event driven hybrid routing protocol for densely deployed wireless sensor networks, J. Netw. Comput. Appl. 58 (2015) 309–326.
[10] S. Raza, M. Faheem, M. Guenes, Industrial wireless sensor and actuator networks in industry 4.0: exploring requirements, protocols, and challenges—A MAC survey, Int. J. Commun. Syst. 32 (15) (2019) e4074.